Immunohistochemistry-quantified EGFR mutant protein expression percentage outperforms next-generation sequencing-derived mutational abundance for predicting tyrosine kinase inhibitor efficacy in non-small cell lung cancer

BOXUAN XIANG[1,2], QI ZHOU[3] and RONGRONG XIE[2]

[1]Graduate School, Jinzhou Medical University, Jinzhou, Liaoning 121001, P.R. China; [2]People's Hospital of Xiangxi Tujia and Miao Autonomous Prefecture, The First Affiliated Hospital of Jishou University Medical College, Xiangxi Tujia and Miao Autonomous Prefecture, Hunan 416000, P.R. China; [3]Department of Oncology, Fuling Hospital Affiliated to Chongqing University, Chongqing 408000, P.R. China

Received June 16, 2026; Accepted October 15, 2026

DOI: 10.3892/ol.2026.15945

Abstract. Epidermal growth factor receptor (EGFR) tyrosine kinase inhibitors (TKIs) are the standard first-line therapy for EGFR-mutant non-small cell lung cancer (NSCLC), yet treatment efficacy varies widely among patients. The aim of the present study was to investigate the correlation between immunohistochemistry (IHC)-quantified EGFR mutant protein expression percentage (MPEP) in tumour tissue and EGFR-TKI efficacy, as well as the clinical predictive value of this mutation percentage. The present retrospective study included 50 patients with NSCLC with EGFR exon 19 deletion or leucine-to-arginine substitution at codon 858 mutations who received EGFR-TKI treatment. IHC was performed to quantify the percentage of EGFR-mutant tumour cells, and the association between this mutation percentage and progression-free survival (PFS), overall survival (OS) and objective response rate (ORR) was analysed. The median IHC-MPEP was 51.18%, with an overall ORR of 50% in the cohort. Receiver operating characteristic curve analysis identified 52.66% as the optimal cut-off value for efficacy prediction. Patients in the high mutation percentage group (≥52.66%; n=24) had a significantly longer median PFS (21.0 vs. 8.5 months; P<0.05) and OS (30 vs. 18 months; P=0.023), as well as a higher ORR (70.8 vs. 30.7%; P=0.004), compared with the low mutation percentage group. The EGFR mutation percentage was confirmed as an independent prognostic factor for PFS (hazard ratio=0.946; 95% confidence interval, 0.927-0.966; P<0.001). Therefore, IHC-MPEP is a reliable quantitative method that can effectively predict EGFR-TKI efficacy and survival benefit in patients with EGFR-mutant NSCLC.

Correspondence to: Professor Qi Zhou, Department of Oncology, Fuling Hospital Affiliated to Chongqing University, 2 Gaosuntang Road, Fuling, Chongqing 408000, P.R. China
E-mail: qizhou112@163.com

Abbreviations: CI, confidence interval; CR, complete response; Del19, exon 19 deletion; FDR, false discovery rate; HR, hazard ratio; IHC, immunohistochemistry; MPEP, mutant protein expression percentage; L858R, leucine-to-arginine substitution at codon 858; NGS, next-generation sequencing; NSCLC, non-small cell lung cancer; ORR, objective response rate; OS, overall survival; PFS, progression-free survival; PR, partial response; ROC, receiver operating characteristic; SD, stable disease; TKI, tyrosine kinase inhibitor

Key words: NSCLC, EGFR, IHC, TKI, PFS

Introduction

Lung cancer remains the leading cause of cancer-related mortality worldwide (1,2), with a particularly heavy disease burden in China, where incidence and mortality continue to rise. In 2022, lung cancer in China accounted for 22.0% of all new cancer cases (n=1,060,600) and 28.5% of all cancer-related mortalities nationwide (3,4). Non-small cell lung cancer (NSCLC) accounts for 85% of all lung cancer cases, primarily comprising lung adenocarcinoma (LUAD) and lung squamous cell carcinoma subtypes, and is frequently diagnosed at advanced stages that are not amenable to surgical resection (5). EGFR mutations, which are detectable in 15-20% of patients with NSCLC, predominantly in LUAD among Asian females and never-smokers (6,7), are key oncogenic drivers of NSCLC (8).

EGFR tyrosine kinase inhibitors (TKIs) inhibit EGFR tyrosine kinase activity, thereby suppressing the downstream RAS-RAF-MEK-ERK proliferative pathway and PI3K-AKT-mTOR pro-survival pathway (9). These agents block ligand-dependent signal initiation and inhibit tumour growth at the molecular level. Clinically, EGFR-TKIs provide markedly superior progression-free survival (PFS) compared with conventional chemotherapy. For example, osimertinib achieves a PFS of 18-19 vs. 5-6 months with chemotherapy (10-12), establishing EGFR-TKIs as the standard first-line therapy for advanced EGFR-mutant NSCLC (13).

Beyond the canonical RAS-RAF-MEK-ERK and PI3K-AKT-mTOR cascades, emerging evidence highlights the involvement of additional signalling axes, such as the JAK-STAT, Wnt/β-catenin and Notch pathways, in mediating tumour progression and treatment resistance (14-17). These pleiotropic mechanisms underscore the complexity of EGFR-driven oncogenesis and the need for comprehensive biomarker strategies that integrate protein-level quantification with genomic profiling.

Despite these therapeutic advances, major challenges remain in predicting EGFR-TKI efficacy. First-line EGFR-TKI therapy exhibits marked heterogeneity in PFS (18), with some patients achieving durable long-term remission, while others experience rapid disease progression (19). This variability is partially attributed to intratumoural heterogeneity, characterised by the coexistence of tumour clones harbouring driver and non-driver mutations (20,21). This phenomenon may be closely related to the percentage of EGFR-mutant tumour cells, which can be quantified using immunohistochemistry (IHC) analysis. A higher mutation percentage likely indicates more robust activation of the EGFR signalling pathway and reduced tumour heterogeneity. By contrast, a lower mutation percentage may reflect compensatory activation of wild-type EGFR or aberrant activation of alternative bypass pathways, such as MET proto-oncogene, receptor tyrosine kinase (MET) amplification, thereby compromising TKI efficacy (22,23). Current bulk next-generation sequencing (NGS), the standard clinical method for EGFR mutation detection, provides only indirect estimates of average mutation allele frequency across the entire tumour specimen and fails to resolve the spatial and temporal dynamics of clonal evolution during EGFR-TKI therapy (24). Importantly, the impact of the percentage of EGFR-mutant tumour cells within the tumour microenvironment on TKI efficacy remains poorly characterised.

IHC is a reliable method as it enables direct cellular quantification and spatial localisation of mutant EGFR protein with high specificity, sensitivity and morphological correlation (25). Accordingly, the present study aimed to quantify the percentage of EGFR-mutant tumour cells in NSCLC tissue samples using mutation-specific IHC and to investigate the correlation between this IHC-quantified EGFR mutant protein expression percentage (MPEP) and EGFR-TKI efficacy, as well as its clinical value as a predictive biomarker in patients with EGFR-mutant NSCLC.

Materials and methods

Clinical information. The present study was a retrospective, non-interventional study using de-identified clinical data and archived pathological specimens. A total of 50 patients with pathologically confirmed NSCLC were included. All patients received EGFR-TKI treatment at the People's Hospital of Xiangxi Tujia and Miao Autonomous Prefecture (The First Affiliated Hospital of Jishou University Medical College), Xiangxi, China, between February 2016 and October 2024. These patients harboured NGS-confirmed EGFR mutations (L858R or Del19) in their pretreatment tumour specimens. Formalin-fixed paraffin-embedded (FFPE) tumour specimens were obtained from the Department of Pathology of the People's Hospital of Xiangxi Tujia and Miao Autonomous Prefecture. Notably, only 24 of the 50 patients underwent valid NGS assessment of EGFR mutation abundance. The remaining 26 patients were excluded from NGS-related analyses because of insufficient residual tumour tissue for NGS library construction, failed NGS testing or low tumour cellularity. The NGS subgroup comprised patients with valid IHC results and complete NGS-derived EGFR mutation abundance data, whereas patients with unavailable NGS reports or inadequate specimen quality were excluded.

Objective tumour responses were assessed every 8 weeks using chest and abdominal computed tomography, brain magnetic resonance imaging and routine laboratory investigation, in accordance with the Response Evaluation Criteria in Solid Tumors (RECIST) version 1.1 (26). PFS was defined as the interval between EGFR-TKI initiation and radiographically confirmed disease progression or death from any cause, whichever occurred first. Overall survival (OS) was defined as the interval between EGFR-TKI initiation and death from any cause. ORR was calculated as the percentage of patients who achieved a complete response (CR) or partial response (PR).

IHC for EGFR L858R or Del19 expression. All tissue specimens were routinely fixed in 10% neutral buffered formalin (pH 7.4) and processed into FFPE blocks according to standard clinical pathology protocols. For routine paraffin section processing, 5-μm-thick sections were first deparaffinised in xylene (2x10 min) and rehydrated through a graded ethanol series, then rinsed in distilled water. Antigen retrieval was then performed using citrate buffer (pH 6.0; cat. no. ZLI-9065; ZSGB-BIO, Beijing, China) in a pressure cooker at 121˚C and 103 kPa for 3 min. After cooling to room temperature for 30 min, endogenous peroxidase activity was blocked by incubating sections at room temperature for 15 min with 3% H_2O_2 in methanol, freshly prepared by diluting 30% H_2O_2 with methanol at a 1:9 (v/v) ratio. Sections were washed three times with PBS (5 min per wash) and blocked with 5% BSA (cat. no. B2064; MilliporeSigma) in PBS at 37˚C for 30 min to minimise non-specific binding.

Immunostaining was performed using the UltraPATH fully automated IHC stainer (ZSGB-BIO, Beijing, China). The primary antibodies used were anti-EGFR L858R monoclonal antibody (cat. no. 26082; Wuhan NewEast Biosciences Co., Ltd.) and anti-EGFR exon 19 deletion (Del19, E746-A750del) monoclonal antibody (cat. no. 26235; Wuhan NewEast Biosciences Co., Ltd.). Both antibodies were diluted 1:100 and incubated with tissue sections overnight at 4˚C. Normal lung tissue known to express wild-type EGFR served as a negative control to verify the specificity of the mutation-specific antibodies. Quantitative analysis of IHC staining was performed using ImageJ (version 1.53k; National Institutes of Health), and the percentage of positively stained area (DAB-positive region) was calculated for each specimen. Each IHC run included a blank control in which the primary antibody was omitted to verify the specificity of the secondary antibody and detection system.

The sections were equilibrated to room temperature for 30 min and washed three times with PBS (5 min per wash). A reaction enhancement solution (cat. no. ZLI-9030; ZSGB-BIO, Beijing, China) was applied, and sections were incubated at 37˚C for 40 min. After three PBS washes, HRP-conjugated

goat anti-mouse IgG secondary antibody (cat. no. ZLI-9028; ZSGB-BIO) was applied at 1:200, and sections were incubated at 37˚C for 60 min. After a further wash (PBS, 3x5 min), chromogenic development was performed using a DAB kit (cat. no. ZLI-9017; ZSGB-BIO, Beijing, China). Colour development was monitored under a light microscope and terminated by immersion in distilled water once the desired staining intensity had been achieved, typically after 3-5 min. Sections were counterstained with haematoxylin staining solution for 90 sec, differentiated with hydrochloric acid-ethanol ultrafast differentiating solution (cat. no. ZLI-9612; ZSGB-BIO, Beijing, China) for 1 sec and blued with 1% lithium carbonate solution. Finally, sections were dehydrated through a graded ethanol series (70, 80, 95 and 100%; 2 min each), cleared in xylene and mounted with neutral balsam.

After slide preparation, digital images were acquired using the Motic Digital Slide Assistant System (MoticEasyScan Pro; Motic Incorporation, Ltd.). A total of five non-overlapping fields were randomly selected from each section and imaged under a 20X objective using a DM2500 microscope (Leica Microsystems, GmbH). ImageJ software was used to quantify the percentage of positively stained brown-yellow area relative to the total tumour area in each field. The mean value across the five fields was calculated and recorded as the final EGFR expression percentage for each specimen. Positive staining was defined as specific brown-yellow staining in ≥10% of tumour cells.

Scoring criteria for EGFR staining intensity. The staining intensity and positive rate of EGFR mutation-specific IHC were independently evaluated by two trained researchers who received specific training in IHC scoring under the supervision of a senior pathologist prior to the study. Both evaluators were blinded to the patients' clinical information and outcomes. Any discrepancies were resolved through discussion. Staining intensity and the positive rate of EGFR mutation-specific IHC were scored according to the following criteria. Staining intensity was scored as follows: 0, no staining or only non-specific staining at the target site; 1, light yellow staining; 2, tan-yellow staining; and 3, brown staining. For positive area scoring, it was scored as follows: 0, 0-10; 1, 10-50; 2, 50-75 and 3, 75-100%. The final EGFR staining grade was categorised into four grades based on the product of the staining intensity and positive rate scores: Grade 0, 0; grade 1, 1-3; grade 2, 4-6; and grade 3, 7-9.

Statistical analysis. PFS was defined as the time from initiation of EGFR-TKI treatment to radiographically confirmed disease progression or death from any cause. OS was defined as the time from EGFR-TKI initiation to death from any cause. ORR was calculated according to the Response Evaluation Criteria in Solid Tumors (RECIST) version 1.1.

All statistical analyses were performed using SPSS 27.0 (IBM Corp.) and R software (version 4.4.1; Posit Software, PBC.). A two-sided P<0.05 was considered to indicate a statistically significant difference. The normality of continuous variables was assessed using the Shapiro-Wilk test. Between-group comparisons of normally distributed continuous variables were performed using the independent-samples Student's t-test, whereas the Mann-Whitney U test was used for non-normally distributed data. Spearman's rank correlation analysis was performed to assess associations between EGFR mutation metrics and clinical outcomes. For multiple comparisons, the Benjamini-Hochberg false discovery rate (FDR) method was applied, and adjusted P-values <0.05 were considered statistically significant. PFS and OS were estimated using the Kaplan-Meier method and compared between groups using the log-rank test. Patients alive at the final follow-up were censored. Univariate and multivariable Cox proportional hazards regression analyses were performed to identify independent prognostic factors. For the univariate Cox analysis, IHC-MPEP was dichotomized into high (≥52.66%) and low (<52.66%) groups based on optimal cut-off value determined by the Youden index via ROC curve analysis, with the low group as the reference. A multivariable Cox proportional hazards regression model was constructed using the Enter method, with IHC-MPEP treated as a continuous variable (per 1% increase) and adjusted a priori for smoking status, brain metastases and EGFR mutation subtype. The proportional hazards assumption was evaluated using Schoenfeld residual tests. Observed statistical power for the two-group log-rank test was estimated using the asymptotic Schoenfeld approximation (27) (Table SI).

Results

Clinical data. Of the 50 enrolled patients, the median age was 60 years (range, 38-85 years), 33 were female (66%) and 33 were never-smokers (66%). All patients had pathologically confirmed LUAD (100%). According to the 8th edition of the TNM staging system (28), 43 patients (86%) had stage IV disease, and 7 patients (14%) had stage III disease at baseline (EGFR-TKI initiation). Baseline brain metastases were present in 15 patients (30%). Regarding EGFR mutation subtypes, 33 patients (66%) harboured Del19 mutations, whereas 17 patients (34%) harboured L858R mutations.

Objective tumour response was assessed in all 50 patients according to RECIST version 1.1. No patient achieved a CR, whereas PR, stable disease (SD) and progressive disease were observed in 25 (50%), 22 (44%) and 3 (6%) patients, respectively. The ORR was 50% (25/50). The median PFS for the entire cohort was 13.0 months, and the median OS was 23.0 months. Regarding EGFR-TKI treatment, most patients received first- or second-generation TKIs (n=39, 78.0%; including icotinib, gefitinib and erlotinib), whereas 11 patients (22.0%) received third-generation TKIs (osimertinib or aumolertinib). Although various EGFR-TKIs were administered, the distribution of specific agents was skewed (for example, erlotinib, n=1). Therefore, statistical comparisons were not performed between individual agents (Table I).

EGFR monoclonal antibody L858R and Del19 IHC staining results. A total of 50 pathological specimens were used for IHC analysis of EGFR mutation percentage using L858R- and Del19-specific monoclonal antibodies. In these specimens, mutant EGFR protein was predominantly localised to the cytoplasm and cell membrane, and adjacent non-neoplastic cells (including stromal cells and normal lung epithelial cells) showed no positive staining. All 50 patients had NGS-verified EGFR L858R or Del19 mutations in their pretreatment tumour specimens. However, valid NGS-derived mutation abundance data were available for only 24 patients because of insufficient

Table I. Patient characteristics (n=50).

Characteristics	Value	Percentage of patients
Age, years		
Median	60	-
Range	38-85	-
Sex		
Male	17	34
Female	33	66
Smoking status		
Never smoker	33	66
Former/current smoker	17	34
Types of EGFR mutations		
Exon 19 deletion	33	66
Leucine-to-arginine substitution at codon 858	17	34
TNM stage		
IV	43	86
III	7	14
Brain metastases		
Brain metastases	15	30
No brain metastases	35	70
Line of TKI therapy		
First	43	86
Second, third	7	14
EGFR-TKI drug type		
First-generation: Icotinib, Gefitinib or Erlotinib	39	78
Third-generation: Osimertinib and aumolertinib	11	22
EGFR-TKI efficacy		
Complete remission	0	0
Partial remission	25	50
Stable disease	22	44
Progressive disease	3	6

TKI, tyrosine kinase inhibitor.

residual tumour tissue for NGS library construction, failed NGS analysis or low tumour cellularity. Positive and negative staining regions coexisted within the same tissue sample, and the proportion of positive staining varied among samples. These findings indicated that mutant and non-mutant clones coexisted within the same patient and that the proportion of EGFR mutations varied among patients. IHC staining showed concordance between these mutation-specific antibodies and NGS testing for detecting EGFR Del19 and L858R mutations in this cohort. Representative results are shown in Fig. 1.

Comparison of IHC-detected EGFR mutation percentage, NGS-derived mutational abundance and traditional IHC staining scoring. Using FFPE tumour tissue sections from 24 enrolled patients with confirmed EGFR Del19 or L858R mutations, a paired comparative analysis was performed using three EGFR mutation quantification metrics: IHC-quantified EGFR mutation percentage, NGS-derived EGFR mutation abundance and conventional IHC staining intensity score. IHC quantification was performed using an EGFR L858R-specific mouse monoclonal antibody and a Del19-specific mouse monoclonal antibody.

Between-metric difference analysis. Before application of the paired-samples Student's t-test, the normality of differences between paired measurements was assessed using the Shapiro-Wilk test. Subsequently, a paired-samples Student's t-test was performed to compare IHC-detected EGFR mutation percentage with NGS-derived mutation abundance. The results showed that the IHC-detected EGFR mutation percentage was significantly higher than the NGS-derived mutation abundance, with a mean difference of 14.949% [95% confidence interval (CI), 4.247-25.651; t=2.738; degrees of freedom (df)=23]. The mean IHC-detected EGFR mutation percentage was 42.05%, whereas the mean NGS-derived mutation abundance was 27.101%.

Inter-method consistency analysis. Bland-Altman analysis was performed to evaluate quantitative agreement between IHC-detected EGFR mutation percentage and NGS-derived mutation abundance. The mean difference between the two metrics was 14.949 (95% CI, 4.247-25.651), with wide 95% limits of agreement (LoA) ranging from -37.479-67.377. The repeatability coefficient was 59.099 (Table SII). These wide 95% LoA values indicated substantial systematic bias between the two methods, suggesting that they should not be used interchangeably for absolute quantification of EGFR mutation burden in clinical practice (Fig. 2).

Rank consistency analysis of multiple mutation metrics. Kendall's W test was performed to assess rank concordance among the three mutation-related metrics: IHC-detected EGFR mutation percentage, NGS-derived mutation abundance and IHC staining intensity score. The analysis demonstrated a significant, moderate level of concordance among the three metrics (W=0.771; χ^2=37; Table SIII).

These findings indicate that, although NGS-derived mutation abundance and IHC-quantified mutant protein expression exhibited significant rank-order concordance, substantial systematic bias existed between the two measures, rendering their absolute quantitative values non-interchangeable. Therefore, NGS-derived mutation abundance should not be interpreted as a direct surrogate for the proportion of EGFR-mutant tumour cells measured by IHC.

Correlation between EGFR mutation percentage and survival outcomes. The Shapiro-Wilk test was used to assess the normality of IHC-detected EGFR mutation percentage, NGS-derived EGFR mutation abundance, PFS and OS. The results showed that IHC-detected EGFR mutation percentage and NGS-derived EGFR mutation abundance were normally distributed, whereas PFS and OS were not (Table SIV).

Accordingly, Spearman rank correlation analysis was performed to evaluate the association between each EGFR mutation metric and clinical survival outcomes. After Benjamini-Hochberg FDR correction for multiple comparisons, IHC-detected EGFR mutation percentage remained significantly positively associated with PFS (Spearman's ρ=0.710).

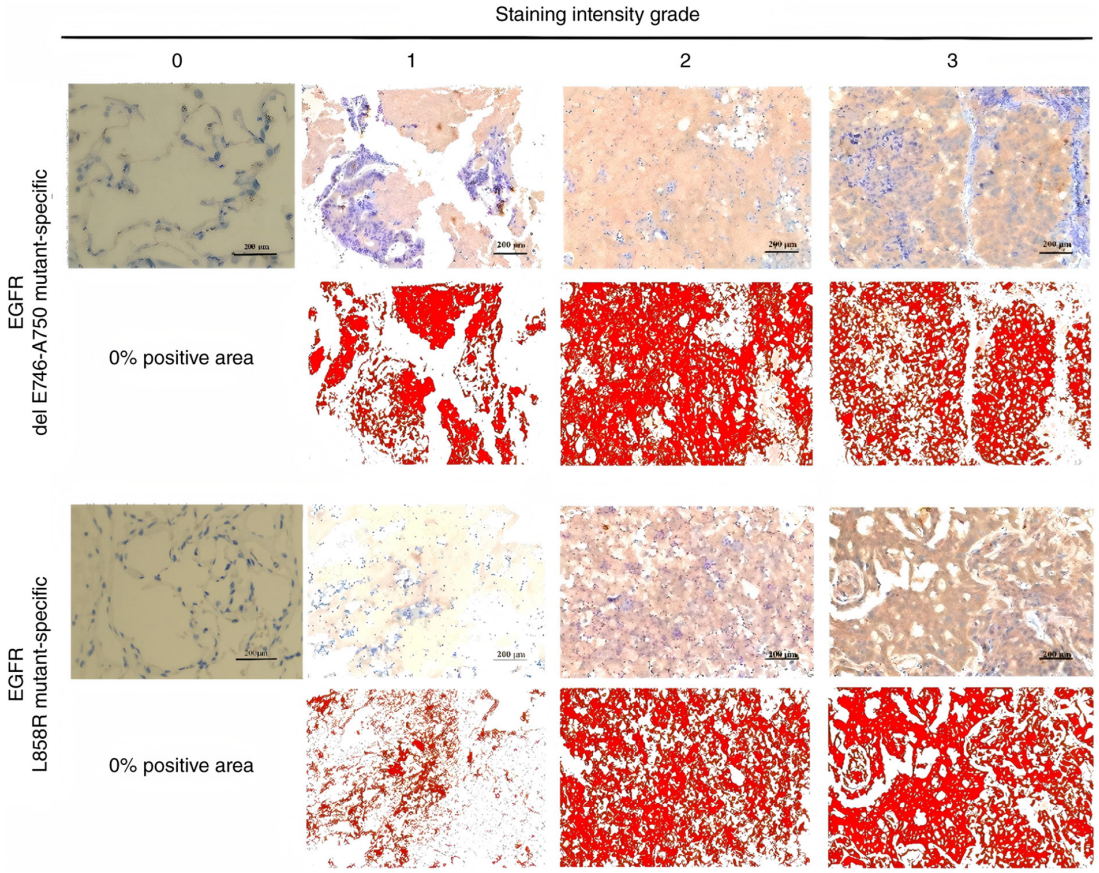


Figure 1. Representative IHC staining and corresponding quantitative analysis of EGFR mutant-specific proteins in non-small cell lung cancer tissues. The columns represent staining intensity grades: Grade 0, negative control using normal lung tissue, showing no mutant EGFR expression; Grade 1, weak; Grade 2, moderate; and Grade 3, strong. The first and third rows show representative IHC images of EGFR del E746-A750 and EGFR L858R mutant proteins, respectively, while the second and fourth rows show their corresponding quantitative analysis images generated in ImageJ, where red areas represent positively stained regions (EGFR mutant protein expression). The normal lung tissue negative control shows 0% positive area, confirming the specificity of the mutant-specific antibodies and ruling out cross-reactivity with wild-type EGFR. Scale bar, 200 μm. EGFR, epidermal growth factor receptor; IHC, immunohistochemistry; L858R, leucine-to-arginine substitution at codon 858.

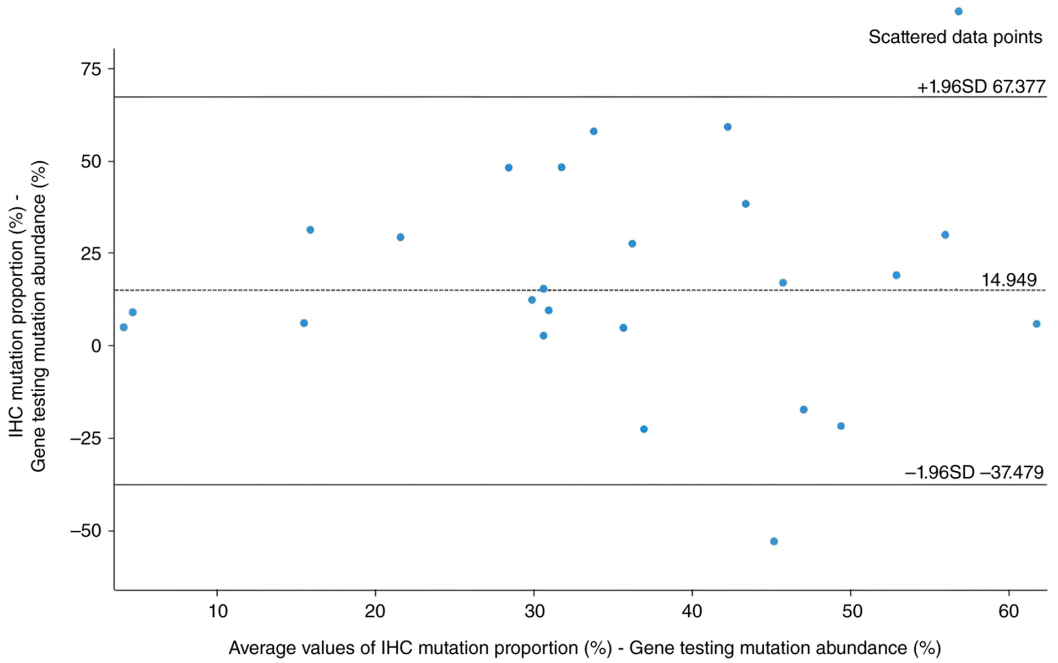


Figure 2. Bland-Altman plot comparing IHC-quantified EGFR mutant protein expression percentage and next-generation sequencing-derived mutation abundance. The solid line indicates the mean difference, and dashed lines indicate the 95% limits of agreement. IHC, immunohistochemistry; SD, standard deviation.

However, its association with OS was no longer statistically significant following FDR correction (Spearman's ρ=0.384). By contrast, NGS-derived EGFR mutation abundance was not significantly associated with either PFS (Spearman's ρ=0.106) or OS (Spearman's ρ=0.151). Furthermore, IHC EGFR staining intensity score was significantly associated with IHC-detected EGFR mutation percentage (Spearman's ρ=0.588), but not with NGS-derived mutation abundance (Spearman's ρ=-0.054; Table II).

Within the entire cohort, 33 patients (66%) harboured EGFR Del19 mutations and 17 patients (34%) harboured EGFR L858R mutations. The distribution of IHC-detected EGFR mutation percentage was compared between these two mutation subtypes. Normality was confirmed for both the Del19 and the L858R (Table SIV). An independent-samples Student's t-test showed no statistically significant difference in mean IHC-detected EGFR mutation percentage between the two groups (Table SV; Fig. 3). These findings suggest that baseline mutant EGFR protein expression quantified by IHC is comparable between the two principal classical EGFR mutation subtypes in the present cohort.

Univariate Cox proportional hazards regression analysis demonstrated that IHC-MPEP was the only variable significantly associated with both PFS (HR=0.19, 95% CI: 0.09-0.38) and OS (HR=0.42, 95% CI: 0.20-0.88), whereas smoking status, brain metastases and EGFR mutation subtype were not significantly associated with either outcome (Table SVI). A multivariable Cox proportional hazards regression analysis was subsequently performed using the Enter method. IHC-MPEP was treated as a continuous variable (per 1% increase), with a priori adjustment for smoking status, brain metastases and EGFR mutation subtype. The analysis confirmed that IHC-MPEP remained an independent prognostic factor for PFS (HR=0.946, 95% CI, 0.927-0.966; Table III). Notably, when analysed as a continuous variable, IHC-MPEP was not significantly associated with OS in the multivariable model (HR=0.988, 95% CI, 0.971-1.005), suggesting a possible threshold effect rather than a linear association for OS prediction. Schoenfeld residual testing supported the proportional hazards assumption for IHC-MPEP (PFS, P=0.101; OS). The present retrospective study did not systematically document performance status, so it was unavailable for adjustment.

Collectively, the present findings indicate that IHC-based quantification of EGFR mutation percentage provides greater predictive value for EGFR-TKI treatment response and survival outcomes in patients with NSCLC than NGS-derived mutation abundance or conventional IHC staining intensity scoring. In addition, IHC-MPEP was identified as an independent prognostic factor for PFS in patients with EGFR-mutant NSCLC receiving EGFR-TKI therapy.

EGFR mutation percentage predicts TKI efficacy. The IHC-detected EGFR mutation percentage showed a statistically significant positive correlation with ORR (Spearman's ρ=0.316), but this association was no longer significant after FDR correction. By contrast, NGS-derived EGFR mutation abundance showed no significant correlation with ORR (Spearman's ρ=0.260; Table II).

Subgroup analysis was subsequently performed in patients stratified according to their best overall response to EGFR-TKI

Table II. Correlation of multifactorial analysis of assays with the efficacy of EGFR-tyrosine kinase inhibitor.

Variable	Progression-free survival time, months			Overall survival time, months			Objective response rate			IHC EGFR staining intensity score		
	Spearman's ρ	P-value	P_FDR	Spearman's ρ	P-value	P_FDR	Spearman's ρ	P-value	P_FDR	Spearman's ρ	P-value	P_FDR
IHC EGFR mutation percentage	0.710	<0.001[a]	<0.008[a]	0.384	0.033[b]	0.066	0.316	0.025[b]	0.066	0.588	0.003[c]	0.012[b]
Next-generation sequencing EGFR mutation abundance	0.106	0.623	0.731	0.151	0.640	0.731	0.260	0.220	0.352	-0.054	0.800	0.800

[a]P<0.001, [b]P<0.05, [c]P<0.01. P-values were determined using Spearman's correlation analysis. P_FDR values were adjusted for multiple comparisons using the Benjamini-Hochberg procedure. IHC, immunohistochemistry; EGFR, epidermal growth factor receptor.

Table III. Multivariable Cox proportional hazards regression analysis of prognostic factors for PFS and OS.

Variable	PFS (n=50)		OS (n=31)	
	HR (95% CI)	P-value	HR (95% CI)	P-value
IHC-MPEP, per 1% increase	0.946 (0.927-0.966)	<0.001[a]	0.988 (0.971-1.005)	0.162
Smoking status, ever vs. never	1.205 (0.610-2.383)	0.591	0.759 (0.321-1.794)	0.530
Brain metastases, yes vs. no	0.734 (0.368-1.462)	0.379	0.749 (0.295-1.901)	0.543
EGFR mutation subtype, leucine-to-arginine substitution at codon 858 vs. exon 19 deletion	1.077 (0.551-2.103)	0.828	1.091 (0.440-2.702)	0.851

Multivariate Cox proportional hazards regression analysis was performed using the Enter method, pre-specified to adjust for the clinically relevant covariates (smoking status, brain metastases and EGFR mutation subtype). IHC-MPEP was treated as a continuous variable (per 1% increase) to maximize statistical power in the multivariable model. [a]P<0.001. IHC-MPEP, immunohistochemistry-quantified EGFR mutant protein expression percentage; HR, hazard ratio; CI, confidence interval; PFS, progression-free survival; OS, overall survival.

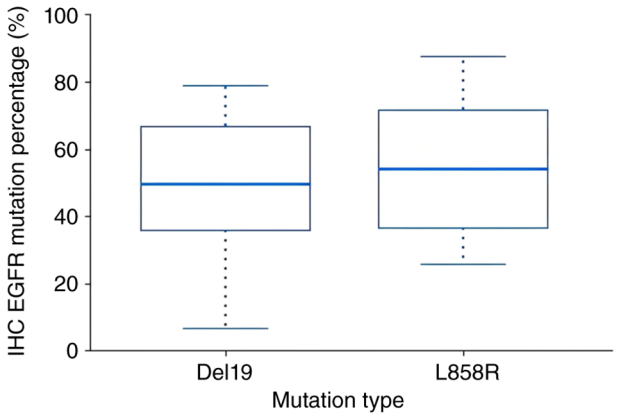


Figure 3. Distribution of IHC-quantified EGFR mutant protein expression between EGFR Del19 and L858R subgroups. No significant difference was observed between groups. IHC, immunohistochemistry; EGFR, epidermal growth factor receptor; Del19, exon 19 deletion, L858R, leucine-to-arginine substitution at codon 858.

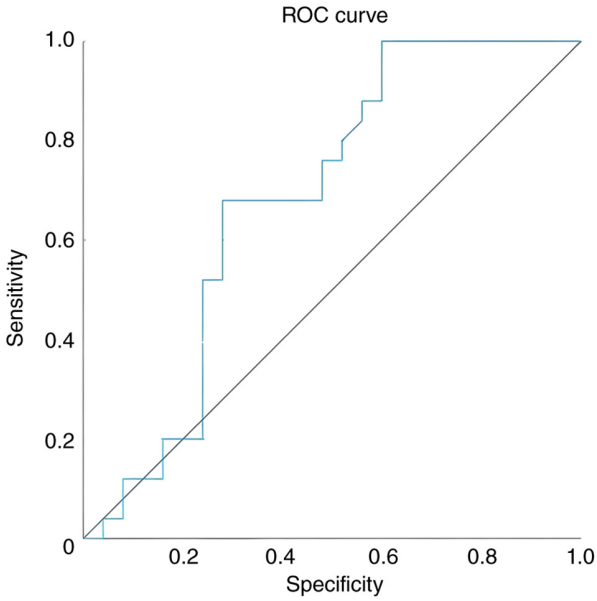


Figure 4. ROC curve for predicting EGFR-tyrosine kinase inhibitor efficacy using immunohistochemistry-quantified EGFR mutant protein expression percentage. The optimal cut-off value was 52.66% (area under the curve, 0.724; 95% confidence interval, 0.583-0.865). ROC, receiver operating characteristic.

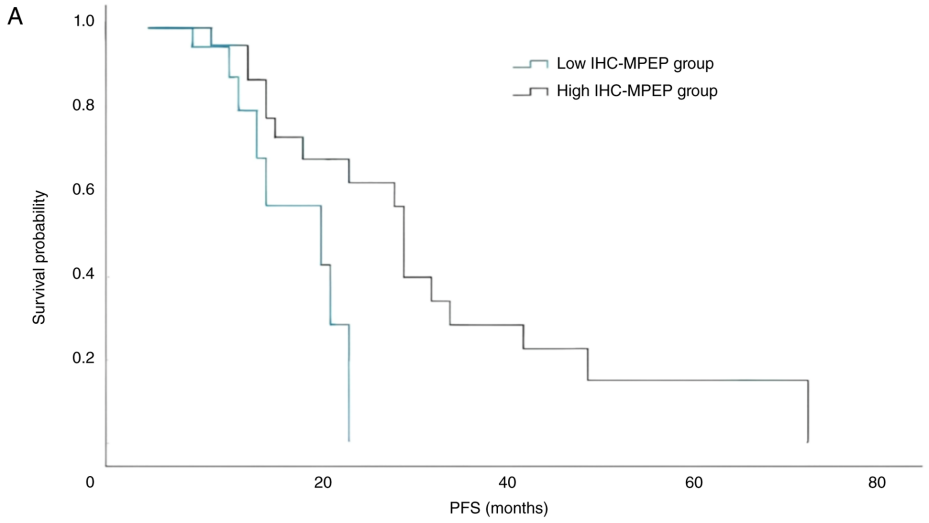
treatment (PR vs. SD). The results showed that IHC-MPEP was significantly higher in the PR group (56.76±14.29%) than in the SD group (44.01±22.45%), with a mean difference of -12.76% (95% CI: -23.507 to -2.005, t=-2.397, df=40.704; Table SVII).

Spearman's rank correlation analysis was subsequently performed to evaluate the association between treatment response metrics (PR/SD) and EGFR mutation quantification results. The analysis revealed no significant association between EGFR-TKI treatment response (PR/SD) and NGS-derived EGFR mutation abundance (Spearman's ρ=0.211). By contrast, EGFR-TKI treatment response was significantly and positively associated with the IHC-detected EGFR mutation percentage (Spearman's ρ=0.361).

Optimal cut-off values of EGFR mutation percentage by IHC and correlation with EGFR-TKI therapeutic efficacy and clinical prognosis. ROC curve analysis identified 52.66% as the optimal cut-off value for the IHC-detected EGFR mutation percentage for predicting EGFR-TKI efficacy, as determined using the Youden index. The analysis yielded an area under the curve of 0.724 (95% CI, 0.583-0.865), with a sensitivity of 72.0% and a specificity of 76.0% (Fig. 4). Patients with an IHC-detected EGFR mutation percentage ≥52.66% were classified as the high mutation percentage group, whereas those with values <52.66% were classified as the low mutation percentage group.

The median PFS was significantly longer in the high than in the low mutation percentage group (21.0 vs. 8.5 months). Similarly, the median OS was significantly longer in the high mutation percentage group than in the low mutation percentage group (30.0 vs. 18.0 months). The overall cohort ORR was 50.0% (25/50). The ORR was 70.8% (17/24) in the high mutation percentage group, compared with 30.7% (8/26) in the low mutation percentage group, representing a significant difference between the groups (Fig. 5).

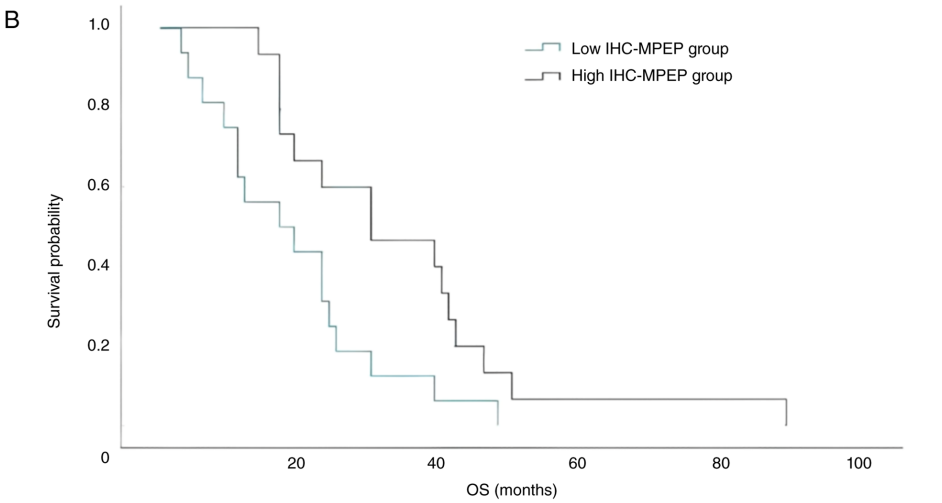
The observed statistical power for the primary PFS endpoint was 100.0% (50 progression events; HR=0.189; 95%



A. Number at risk for progression-free survival (PFS) analysis

Number at risk	0	20	40	60	80
Low IHC-MPEP group	26	3	0	0	0
High IHC-MPEP group	24	13	5	2	0

Time points are in months. All 50 patients had documented progression events. Low IHC-MPEP group, n = 26; High IHC-MPEP group, n = 24.



B. Number at risk for overall survival (OS) analysis

Number at risk	0	20	40	60	80	100
Low IHC-MPEP group	16	7	1	0	0	0
High IHC-MPEP group	15	10	6	1	1	0

Time points are in months. OS analysis included 31 patients with documented death events. Low IHC-MPEP group, n = 16; High IHC-MPEP group, n = 15.

Figure 5. Kaplan-Meier survival curves stratified by IHC-MPEP. (A) PFS (n=50). (B) OS (n=31). Log-rank test revealed significant differences between high and low IHC-MPEP groups. IHC-MPEP, immunohistochemistry-quantified EGFR mutant protein expression percentage; OS, overall survival; PFS, progression-free survival.

CI, 0.094-0.381), substantially exceeding the conventionally accepted threshold of 80% and confirming adequate statistical power for the primary endpoint analysis. For the secondary OS endpoint, observed statistical power was 68.5% (31 death events; HR=0.416; 95% CI, 0.196-0.884), below the 80% threshold (Table SI).

Discussion

As precision oncology advances, molecularly targeted therapy has become a cornerstone of cancer treatment (29). EGFR, a transmembrane tyrosine kinase receptor, is one of the best-characterised oncogenic drivers in NSCLC (30). Its downstream signalling pathways serve pivotal roles in regulating cancer cell proliferation, differentiation and migration (31), making EGFR an established therapeutic target in NSCLC (32). For patients with advanced EGFR-mutant NSCLC, EGFR-TKIs represent the standard first-line treatment and have consistently improved survival outcomes and quality of life (33-35). However, substantial interpatient variability in treatment response and long-term survival remains an important clinical challenge. Although intratumoural

heterogeneity is widely recognised as a major contributor to this variability (20,21), current clinical assessment methods have important limitations. NGS-derived mutation abundance can be affected by tumour cellularity, stromal contamination and necrotic tissue within bulk tumour specimens (24), whereas conventional semi-quantitative IHC scoring is prone to interobserver variability and does not adequately reflect the overall burden of functional mutant EGFR protein (25). In this context, the present study systematically evaluated the predictive value of IHC-MPEP for EGFR-TKI efficacy and performed the first direct comparison of this protein-level metric, conventional IHC staining intensity scoring and NGS-derived genomic mutation abundance within the same patient cohort. IHC-MPEP was an independent prognostic factor for PFS and showed notable associations with OS and ORR when patients were stratified using the ROC-derived optimal cut-off value of 52.66%, suggesting a threshold effect rather than a purely linear association.

These findings are consistent with several landmark studies and extend current knowledge on predictive biomarker development for EGFR-targeted therapy. In agreement with the pivotal study by Azuma *et al* (36), conventional semi-quantitative IHC staining intensity scores for mutant EGFR were significantly associated with PFS in EGFR-TKI-treated NSCLC, but not with OS. The present study further demonstrated that continuous digital quantification of mutant EGFR protein expression can overcome this limitation. IHC-MPEP showed a strong independent association with PFS, together with significant threshold-based associations with OS and ORR. This difference is biologically plausible because conventional semi-quantitative scoring reflects staining intensity within individual tumour cells rather than the overall tumour burden of mutant EGFR protein, whereas IHC-MPEP directly quantifies the expression level of the therapeutic target itself, which is closely associated to the mechanism of action of EGFR-TKIs. A marked positive association was also observed between conventional IHC staining intensity scores and IHC-MPEP, indicating that although both measures reflect mutant EGFR protein expression, continuous percentage-based quantification provides a more comprehensive, reproducible and prognostically informative assessment of EGFR pathway activation within tumour tissue.

Similarly, the present findings are consistent with the landmark study by Zhou *et al* (37), which reported that higher NGS-derived EGFR mutation abundance was associated with prolonged PFS but not with ORR or OS in patients with NSCLC treated with EGFR-TKIs. The present study extends these observations by demonstrating that NGS-derived mutation abundance was not significantly associated with any of the three clinical endpoints in this cohort and showed no significant correlation with IHC-based protein expression metrics. This discrepancy may reflect the inherent limitations of bulk NGS. Bulk sequencing determines the average mutant allele frequency across all cells within a specimen and may therefore be influenced by non-tumour cell contamination, tumour necrosis and low tumour cellularity. In addition, it does not directly reflect the functional expression level of mutant EGFR protein, which represents the immediate therapeutic target of EGFR-TKIs (24). By contrast, IHC-based protein quantification is performed exclusively within histologically confirmed viable tumour regions, thereby minimising these potential confounding factors. Collectively, these exploratory findings suggest that genomic- and protein-level quantification capture distinct biological aspects of EGFR mutation burden. The observed lack of correlation between the two approaches indicates that they may provide complementary rather than interchangeable information for predicting EGFR-TKI efficacy. Larger prospective studies are warranted to directly compare their predictive performance.

ROC curve analysis identified 52.66% as the optimal IHC-MPEP cut-off value for predicting EGFR-TKI efficacy. This threshold effectively stratified patients into distinct prognostic groups. Patients with IHC-MPEP ≥52.66% exhibited a 2.47-fold longer median PFS, a 1.67-fold longer median OS and more than double the ORR compared with those below the threshold. Subgroup analyses by treatment response (PR vs. SD) further supported these findings, showing that higher IHC-MPEP values were associated with a higher likelihood of achieving PR and more favourable survival outcomes. Together, these results suggest that this cut-off may have potential clinical utility for risk stratification beyond a simple prognostic association. From a biological perspective, these observations are consistent with the concept of oncogene addiction, which underpins the therapeutic activity of EGFR-TKIs (38). These findings further suggest that the degree of oncogene addiction may relate to the overall burden of mutant EGFR protein expression within tumour tissue. Higher IHC-MPEP values indicate that a greater proportion of tumour cells is driven by mutant EGFR signalling, potentially resulting in more profound and sustained tumour suppression following EGFR-TKI treatment. Conversely, lower mutant EGFR protein expression may reflect greater intratumoural heterogeneity, with a larger proportion of tumour cells driven by wild-type EGFR signalling or alternative bypass pathways, such as MET amplification and fibroblast growth factor receptor dysregulation, which are recognised mechanisms of primary resistance to EGFR-TKIs (39). These findings complement the established association between genomic EGFR mutation status and EGFR-TKI efficacy by providing a direct protein-level assessment. Accordingly, IHC-MPEP may serve as both a predictive biomarker of EGFR-TKI response and a surrogate indicator of functional EGFR pathway activation.

The clinical and translational feasibility of this biomarker represents a major strength of the present study. Validation using normal lung tissue as a negative control supported the high specificity of the mutation-specific antibodies, which showed 0% positive staining area and no detectable cross-reactivity with wild-type EGFR. These findings further support the reliability of the IHC-based quantification approach. Compared with NGS, IHC-based quantification offers several practical advantages, including technical simplicity, minimal requirements for specialised instrumentation and substantially lower operational costs, estimated at 10-20% of the per-test cost of NGS. Such advantages facilitate implementation in resource-limited community and primary care settings and support the potential utility of IHC-MPEP as a practical tool for predicting EGFR-TKI response across diverse healthcare environments. Importantly, the identified threshold may extend beyond conventional biomarker applications by linking quantitative protein assessment to therapeutic decision-making.

As such, it could support more refined prognostication, cost-effective implementation of precision oncology and individualised treatment selection. Furthermore, given evidence that patients with EGFR-mutant NSCLC derive limited benefit from immune checkpoint inhibitor monotherapy (40), this threshold may help guide initial treatment strategies. Patients with high IHC-MPEP values may be suitable candidates for upfront EGFR-TKI monotherapy, particularly older individuals or those with substantial comorbidity burdens. By contrast, patients with low IHC-MPEP values may require closer surveillance and could potentially benefit from more intensive therapeutic approaches aimed at reducing the risk of primary resistance, although this hypothesis requires prospective validation.

Several limitations should be considered when interpreting these findings. First, this single-centre retrospective study involved a relatively small cohort of 50 patients, which may have introduced selection bias and limited the generalisability of the results. However, the strong independent association observed between IHC-MPEP and PFS supports its potential value as a predictive biomarker. Second, for OS, multivariable analysis treating IHC-MPEP as a continuous variable showed no significant linear association. This finding was likely influenced by the relatively small number of OS events and the resulting limited statistical power. Notably, application of the ROC-derived optimal cut-off value of 52.66% revealed a significant difference in OS by Kaplan-Meier analysis. This observation suggests that the effect of IHC-MPEP on long-term survival may be characterised by a threshold phenomenon, whereby patients with sufficiently high mutant protein expression (≥52.66%) derive greater clinical benefit. Third, the NGS subgroup analysis was limited by the small sample size, reducing power to detect associations with clinical outcomes. Fourth, the distribution of individual EGFR-TKI agents was imbalanced, with some treatments represented by few patients, precluding meaningful comparisons between agents. In addition, owing to the retrospective design and the limited availability of archived specimens, EGFR wild-type tissue was not included as a tissue-based negative control. Instead, a blank control generated by omission of the primary antibody was used. Furthermore, the heterogeneous staining patterns observed within individual tissue sections provided additional support for antibody specificity. Finally, performance status was not systematically documented and was therefore unavailable for inclusion in the multivariable analyses. These limitations emphasise the need for larger, prospectively collected, multicentre studies to validate the clinical utility of IHC-MPEP and its capacity for threshold-based risk stratification.

In conclusion, the present study demonstrates that IHC-quantified EGFR mutant protein expression percentage is a robust, cost-effective and clinically feasible biomarker for predicting EGFR-TKI efficacy and survival outcomes in EGFR-mutant NSCLC. By providing a direct, histologically validated measure of functional EGFR pathway activation, this IHC-based approach complements the genomic information obtained through NGS. Following prospective validation, IHC-MPEP may provide a practical tool for risk stratification and personalised treatment optimisation in patients with EGFR-mutant NSCLC.

Acknowledgements

Not applicable.

Funding

No funding was received.

Availability of data and materials

The data generated in the present study may be requested from the corresponding author.

Authors' contributions

BX and RX jointly performed the immunohistochemical staining evaluation and scoring. BX was responsible for patient screening, specimen collection, immunohistochemical experiments, data sorting and statistical analysis and drafted the original manuscript. QZ conceived and designed the overall research scheme, supervised the entire study process and revised and polished the final manuscript. RX undertook pathological diagnosis, immunohistochemical staining evaluation and result verification. All authors participated in discussing the research results. BX and confirm the authenticity of all the raw data. All authors read and approved the final version of the manuscript.

Ethics approval and consent to participate

The present retrospective, non-interventional clinical study was conducted in accordance with the ethical standards laid down in the 2013 revised Declaration of Helsinki. The Ethics Committee of the People's Hospital of Xiangxi Tujia and Miao Autonomous Prefecture formally reviewed and approved the study protocol (approval no. XXZRY-LCKY-2025-99). All enrolled patients provided written informed consent for the collection of clinical information and the use of archived formalin-fixed paraffin-embedded tumour specimens for this research. All patient data were fully de-identified to protect individual privacy throughout the study.

Patient consent for publication

Written informed consent for the publication of de-identified clinical data, statistical results and anonymized pathological immunohistochemical images was obtained from all enrolled patients.

Competing interests

The authors declare that they have no competing interests.

Use of artificial intelligence tools

During the preparation of this work, artificial intelligence tools were used to improve the readability and language of the manuscript, and subsequently, the authors revised and edited the content produced by the artificial intelligence tools as necessary, taking full responsibility for the ultimate content of the present manuscript.

References

1. Siegel RL, Giaquinto AN and Jemal A: Cancer statistics, 2024. CA Cancer J Clin 74: 12-49, 2024.
2. Sung H, Ferlay J, Siegel RL, Laversanne M, Soerjomataram I, Jemal A and Bray F: Global cancer statistics 2020: GLOBOCAN estimates of incidence and mortality worldwide for 36 cancers in 185 countries. CA Cancer J Clin 71: 209-249, 2021.
3. Wei KR and Chen Y: Cancer registration in the People's Republic of China. Asian Pac J Cancer Prev 13: 4209-4214, 2012.
4. Bray F, Laversanne M, Soerjomataram I, Jemal A and Sung H: Global cancer statistics 2022: GLOBOCAN estimates of incidence and mortality worldwide for 36 cancers in 185 countries. CA Cancer J Clin 74: 227-258, 2024.
5. Hatami E, Nagesh PKB and Ramesh A: Gambogic acid potentiates gemcitabine-induced anticancer activity in non-small cell lung cancer. Eur J Pharmacol 888: 173486, 2020.
6. Bade BC and Dela Cruz CS: Lung cancer 2020: Epidemiology, etiology, and prevention. Clin Chest Med 41: 1-24, 2020.
7. Possenti I, Romelli M, Carreras G, Biffi A, Bagnardi V, Specchia C, Gallus S and Lugo A: Association between second-hand smoke exposure and lung cancer risk in never-smokers: A systematic review and meta-analysis. Eur Respir Rev 33: 240077, 2024.
8. Wu SG and Shih JY: Management of acquired resistance to EGFR-TKI-targeted therapy in advanced non-small cell lung cancer. Mol Cancer 17: 38, 2018.
9. Khaddour K, Jonna S, Deneka A, Patel JD, Abazeed ME, Golemis E, Borghaei H and Boumber Y: Targeting the epidermal growth factor receptor in EGFR-mutated lung cancer: Current and emerging therapies. Cancers (Basel) 13: 3164, 2021.
10. Maemondo M, Inoue A, Kobayashi K, Sugawara S, Oizumi S, Isobe H, Gemma A, Harada M, Yoshizawa H, Kinoshita I, *et al*: Gefitinib or chemotherapy for non-small-cell lung cancer with mutated EGFR. N Engl J Med 362: 2380-2388, 2010.
11. Mitsudomi T, Morita S, Yatabe Y, Negoro S, Okamoto I, Tsurutani J, Seto T, Satouchi M, Tada H, Hirashima T, *et al*: Gefitinib versus cisplatin plus docetaxel in patients with non-small-cell lung cancer harbouring mutations of the epidermal growth factor receptor (WJTOG3405): An open label, randomised phase 3 trial. Lancet Oncol 11: 121-128, 2010.
12. Soria JC, Ohe Y, Vansteenkiste J, Reungwetwattana T, Chewaskulyong B, Lee KH, Dechaphunkul A, Imamura F, Nogami N, Kurata T, *et al*: Osimertinib in untreated EGFR-mutated advanced non-small-cell lung cancer. N Engl J Med 378: 113-125, 2018.
13. Gomez-Randulfe I, Scanlon LA, Carter M, Moliner L, Cil E, Califano R, Summers Y, Blackhall F, Lindsay CR, Lewis J and Gomes F: First-line osimertinib compared to earlier generation TKIs in advanced EGFR-mutant NSCLC: A real-world survival analysis. Lung Cancer 200: 108084, 2025.
14. Samant C, Kale R, Pai KSR, Nandakumar K and Bhonde M: Role of Wnt/β-catenin pathway in cancer drug resistance: Insights into molecular aspects of major solid tumors. Biochem Biophys Res Commun 729: 150348, 2024.
15. Bousquet Mur E, Bernardo S, Papon L, Mancini M, Fabbrizio E, Goussard M, Ferrer I, Giry A, Quantin X, Pujol J-L, *et al*: Notch inhibition overcomes resistance to tyrosine kinase inhibitors in EGFR-driven lung adenocarcinoma. J Clin Invest 130: 612-624, 2020.
16. Du Z, Kan H, Sun J, Liu Y, Gu J, Akemujiang S, Zou Y, Jiang L, Wang Q, Li C, *et al*: Molecular mechanisms of acquired resistance to EGFR tyrosine kinase inhibitors in non-small cell lung cancer. Drug Resist Updat 82: 101266, 2025.
17. Hu X, Li J, Fu M, Zhao X and Wang W: The JAK/STAT signaling pathway: from bench to clinic. Signal Transduct Target Ther 6: 402, 2021.
18. Yan H, Peng J, Zhou W, Chen H and He C: Correlation analysis of EGFR gene mutation abundance and the efficacy of osimertinib in nonsmall cell lung cancer: A case control study. J Oncol Pharm Pract 31: 175-181, 2025.
19. Hu W, Qin Y, Dong T, Lin X and Chen Y: Third generation vs first generation EGFR-TKIs in the first line treatment for EGFR-mutated locally advanced or metastatic non-small cell lung cancer: A meta-analysis based on randomized controlled trials. J Cancer 16: 735-747, 2025.
20. Qiu Y, Liu L, Yang H, Chen H, Deng Q, Xiao D, Lin Y, Zhu C, Li W, Shao D, *et al*: Intratumor heterogeneity of driver mutations and TMB distribution in 30 early-stage LUAD patients with multiple lesions. Front Oncol 12: 952572, 2022.
21. Morjaria S: Driver mutations in oncogenesis. Int J Mol Immuno Oncol 6: 100-102, 2021.
22. Buder A, Hochmair MJ and Filipits M: The allele frequency of EGFR mutations predicts survival in advanced EGFR T790M-positive non-small cell lung cancer patients treated with osimertinib. Target Oncol 16:77-84, 2021.
23. Sequist LV, Waltman BA, Dias-Santagata D, Digumarthy S, Turke AB, Fidias P, Bergethon K, Shaw AT, Gettinger S, Cosper AK, *et al*: Genotypic and histological evolution of lung cancers acquiring resistance to EGFR inhibitors. Sci Transl Med 3: 75ra26, 2011.
24. Passaro A, Malapelle U, Del Re M, Attili I, Russo A, Guerini-Rocco E, Fumagalli C, Pisapia P, Pepe F, De Luca C, *et al*: Understanding EGFR heterogeneity in lung cancer. ESMO Open 5: e000919, 2020.
25. Ai X, Cui J, Zhang J, Chen R, Lin W, Xie C, Liu A, Zhang J, Yang W, Hu X, *et al*: Clonal architecture of EGFR mutation predicts the efficacy of EGFR-tyrosine kinase inhibitors in advanced NSCLC: A prospective Multicenter study (NCT03059641). Clin Cancer Res 27: 704-712, 2021.
26. Eisenhauer EA, Therasse P, Bogaerts J, Schwartz LH, Sargent D, Ford R, Dancey J, Arbuck S, Gwyther S, Mooney M, *et al*: New response evaluation criteria in solid tumours: Revised RECIST guideline (version 1.1). Eur J Cancer 45: 228-247, 2009.
27. Schoenfeld DA: The asymptotic properties of nonparametric tests for comparing survival distributions. Biometrika 68: 316-319, 1981.
28. Rami-Porta R, Asamura H, Travis WD and Rusch VW: Lung cancer-major changes in the American Joint Committee on Cancer eighth edition cancer staging manual. CA Cancer J Clin 67: 138-155, 2017.
29. Tibau A, Hwang TJ, Avorn J and Kesselheim AS: Clinical value of guideline recommended molecular targets and genome targeted cancer therapies: Cross sectional study. BMJ 386: e079126, 2024.
30. Imyanitov EN, Iyevleva AG and Levchenko EV: Molecular testing and targeted therapy for non-small cell lung cancer: Current status and perspectives. Crit Rev Oncol Hematol 157: 103194, 2021.
31. Leonetti A, Sharma S, Minari R, et al: Resistance mechanisms to osimertinib in EGFR-mutated non-small cell lung cancer. Br J Cancer 121: 725-737, 2019.
32. Dong RF, Zhu ML, Liu MM, Xu YT, Yuan LL, Bian J, Xia YZ and Kong LY: EGFR mutation mediates resistance to EGFR tyrosine kinase inhibitors in NSCLC: From molecular mechanisms to clinical research. Pharmacol Res 167: 105583, 2021.
33. Moore S and Wheatley-Price P: EGFR combination therapy should become the new standard first-line treatment in advanced EGFR-mutant NSCLC. J Thorac Oncol 16: 1788-1792, 2021.
34. Levantini E, Maroni G, Del Re M and Tenen DG: EGFR signaling pathway as therapeutic target in human cancers. Semin Cancer Biol 85: 253-275, 2022.
35. Nan XL, Xie C, Yu X and Liu J: EGFR TKI as first-line treatment for patients with advanced EGFR mutation-positive non-small-cell lung cancer. Oncotarget 8: 75712-75726, 2017.
36. Azuma K, Okamoto I, Kawahara A, Taira T, Nakashima K, Hattori S, Kinoshita T, Takeda M, Nakagawa K, Takamori S, *et al*: Association of the Expression of Mutant Epidermal Growth Factor Receptor Protein as Determined with Mutation-Specific Antibodies in Non-small Cell Lung Cancer with Progression-Free Survival after Gefitinib Treatment. J Thorac Oncol 7: 122-127, 2012.
37. Zhou Q, Zhang XC, Chen ZH, Yin X-L, Yang J-J, Xu C-R, Yan H-H, Chen H-J, Su J, Zhong W-Z, *et al*: Relative Abundance of EGFR Mutations Predicts Benefit From Gefitinib Treatment for Advanced Non–Small-Cell Lung Cancer. J Clin Oncol 29: 3316-3322, 2011.
38. Wang R, Wei H, Qu C, Bai Y and Zhang W: Unlocking the potential: tissue mutation abundance as a predictor for third-generation EGFR-TKI efficacy in NSCLC. Lung Cancer 207: 108699, 2025.
39. Hu LY, Zhuang WT, Chen MJ, Liao J, Wu DF, Zhang YX, Pang LL, Huang YH, Mao TQ, Yang MJ, *et al*: EGFR mutations impair macrophage phagocytosis. J Thorac Oncol 19: 876-889, 2024.
40. To KKW, Fong W and Cho WCS: Immunotherapy in treating EGFR-mutant lung cancer: Current challenges and new strategies. Front Oncol 11: 635007, 2021.

Copyright © 2026 Xiang et al. This work is licensed under a Creative Commons Attribution-NonCommercial-NoDerivatives 4.0 International (CC BY-NC-ND 4.0) License.